THE ASTROPHYSICAL JOURNAL, 549:90–99, 2001 March 1
© 2001. The American Astronomical Society. All rights reserved. Printed in U.S.A.

UVES OBSERVATIONS OF QSO 0000−2620: ARGON AND PHOSPHORUS ABUNDANCES IN THE DUST-FREE DAMPED Lyα SYSTEM AT $z_{abs} = 3.3901$[1]

PAOLO MOLARO,[2] SERGEI A. LEVSHAKOV,[3] SANDRO D'ODORICO,[4] PIERCARLO BONIFACIO,[2] AND MIRIAM CENTURIÓN[2]

Received 2000 July 31; accepted 2000 October 30

ABSTRACT

The UV resonance transitions of neutral argon, Ar I λ1066, and of singly ionized phosphorus, P II λ963, originated in the damped Lyα system (DLA) at $z_{abs} = 3.3901$ toward QSO 0000−2620, have been detected by means of the Ultraviolet-Visual Echelle Spectrograph (UVES) spectrograph at the 8.2 m ESO KUEYEN telescope. So far, this is the first measurement of Ar I and the second of P II ever performed in damped galaxies and in high-redshift objects. This DLA is well known for having one of the lowest metal abundances and dust content and the lowest fractional abundance of molecular hydrogen H_2. The measured Ar abundance is $[Ar/H] = -1.91 \pm 0.09$, which is equal to the abundances of the other α-chain elements (O, S, and Si). The similarity of the Ar abundance with the other α-chain elements implies the absence of significant photoionization by either UV background or stellar sources along the sight line throughout the damped Lyα system. Both log (Ar/O) and log (Ar/S) ratios are found close to those measured in the extragalactic H II regions and in blue compact galaxies where O is more abundant by at least 1 order of magnitude. This strengthens the universality of the Ar/O and Ar/S ratios and lends support to the existence of a universal IMF. The abundance of the nonrefractory element phosphorus $[P/H] = -2.31 \pm 0.10$ confirms the low amount of chemical evolution in the DLA. This is the measurement of P in the most metal-poor material and shows a subsolar $[P/Fe] = -0.27$ value. The measured ratios $[P/Si] = -0.40 \pm 0.13$ and $[P/S] = -0.40 \pm 0.13$ provide evidence for a mild odd-even effect. Finally, a stringent upper limit to the population of the $^3P_1$ level in the ground state of O I is derived, which provides a lower limit to the physical dimensions of the $z_{abs} = 3.3901$ system of $L > 7$ pc.

Subject headings: cosmology: observations — galaxies: abundances — galaxies: evolution — quasars: absorption lines

Damped Lyα (DLA) systems are absorption systems observed in quasar spectra characterized by large column densities [$N(H\ I) \geq 2 \times 10^{20}$ cm^{-2}]. They span the whole epoch of galaxy formation and are generally considered the progenitors of the present-day galaxies. DLA systems are of particular interest because it is possible to measure a variety of chemical elements in their interstellar gas phase with unprecedented precision (Lu et al. 1996; Prochaska & Wolfe 1999; Pettini et al. 1997, 1999, 2000). However, the observed abundance patterns in the DLAs proved difficult to account for, because of the possibility that a significant fraction of some elements contribute to dust grain formation, thus depleting the gas-phase abundances (Kulkarni et al. 1997; Vladilo 1998). At face value the observed Si, S, Cr, Al, and Ni abundances relative to Fe are similar to those observed in the old stellar population of the Galaxy, with the notable exception of Zn, which is overabundant compared to iron. However, if the [Zn/Fe] *anomaly* is interpreted as a Fe depletion in the interstellar medium, the observed abundance pattern would be similar to those observed in the warm phase of the interstellar medium with solar chemical composition. Zinc has not been considered a totally reliable element by Prochaska et al. (2000), because of its uncertain nucleosynthesis. A sample of chemical elements larger than those presently available, and in particular of elements with little affinity with dust grains, is required to better address the kind of chemical pattern present in DLA systems.

In this paper we report on the detection of UV lines of the nondepleted species-neutral argon, Ar I, and singly ionized phosphorus, P II—in a DLA system at $z_{abs} = 3.3901$ toward the quasar QSO 0000−2620. So far, phosphorus has been measured by Outram et al. (1999) in the DLA system at $z_{abs} = 2.625$ toward GB 1759+7539 and an upper limit on phosphorus abundance has been set for the DLA system at $z_{abs} = 2.309$ toward PHL 957 (Molaro et al. 1998). A possible identification of the Ar I lines in the $z_{abs} = 2.8112$ DLA toward PKS 0528−250 was reported by Srianand & Petitjean (1998); however, in their spectrum the Ar I lines were considerably contaminated by hydrogen absorption, which yields a rather uncertain Ar I column density.

The Ar we derive here is the first one ever obtained in any DLA system and one of the few values measured by means of unsaturated lines, unlike the results of the interstellar studies in the Galaxy (e.g., Sofia & Jenkins 1998). Being a noble gas with very low condensation temperature, $T_c = 30$ K (Spitzer & Jenkins 1975), neutral argon atoms do not form chemical bonds with solid compounds, and the depletion of phosphorus is found to be very small in the interstellar medium (ISM) where variations in refractory elements do occur (e.g., Dufton et al. 1986). The dust-to-gas ratio in the DLA at $z_{abs} = 3.3901$ toward QSO 0000−2620 was found to be less than 0.2% than that in the Milky Way (Levshakov et al. 2000b), and thus the measured [Ar/H]

[1] Based on public data from the UVES Commissioning at the ESO 8.2 m KUEYEN telescope operated on Paranal Observatory, Chile; molaro@oat.ts.astro.it.

[2] Osservatorio Astronomico di Trieste, Via G.B. Tiepolo 11, 34131 Trieste, Italy.

[3] Department of Theoretical Astrophysics, Ioffe Physico-Technical Institute, 194021 St. Petersburg, Russia.

[4] European Southern Observatory, Karl-Schwarzschild-Strasse 2, D-85740 Garching, Germany.

and [P/H] ratios[5] at $z_{abs} = 3.3901$ should not be significantly affected by dust depletion, thus providing a unique probe of pure nucleosynthetic yields at high redshift.

The study of phosphorus may eventually allow clarification of the dust formation processes in DLA galaxies. Since P and Fe have nearly the same condensation temperature $T_c \simeq 1300$ K, these species should deplete together in equal proportions if dust is produced in dense and hot shells of supernova remnants where thermodynamic calculations of condensation are appropriate. A possible disparity between P and Fe gas phase-abundances would favor a different model where the dust grains grow in the interstellar medium (see Jura & York 1978 and references therein).

We discuss here the implications of the Ar and P abundances in connection with the chemical evolution of such damped galaxies. We underline that for research on the element production history, Ar is a quite unique element as a result of its ability to trace how strongly the apparent abundances of other species from H I regions could be influenced by ionization.

The paper is organized as follows: in § 1 we briefly describe observations and analyze Ar I and P II profiles. The results on Ar and P abundances are discussed in § 2 (§§ 2.1 and 2.2, respectively). In § 2.3, the estimations of the mean gas density and the linear size of the $z_{abs} = 3.3901$ system are also given. Conclusions are summarized in § 3.

1. OBSERVATIONS, DATA REDUCTION, AND COLUMN DENSITIES

The DLA system at $z_{abs} = 3.3901$ toward QSO 0000−2620 shows high neutral hydrogen column density $N(\text{H I}) = 10^{21.41 \pm 0.08}$ cm^{-2} (Lu et al. 1996). This system has been studied extensively, since it is one of the highest redshift DLA systems seen in the light of a relatively bright QSO (Levshakov et al. 1992; Molaro et al. 1996; Prochaska & Wolfe 1999; Molaro et al. 2000, hereafter Paper I; Levshakov et al. 2000b, hereafter Paper II).

The spectra of QSO 0000−2620 were obtained during the first commissioning of the Ultraviolet-Visual Echelle Spectrograph (UVES; see Dekker et al. 2000) at the Nasmyth focus of the ESO 8.2 m KUEYEN telescope at Paranal, Chile, in 1999 October, and have been released for public use. Details of observations and of data reduction are given in Paper I. We recall here that the resolving power is $R = \lambda/\Delta\lambda_{instr} \simeq 49{,}000$, which corresponds to a velocity resolution of $\simeq 6$ km s^{-1} (FWHM).

Singly ionized phosphorus, which is the dominant state in H I gas, has three strong UV lines with $\lambda = 961.041$ Å, 963.801, and 1152.818 Å (the corresponding f-values are equal to 0.3489, 1.458, and 0.2361, according to Morton 1991). We have detected with confidence only the P II λ963 line which is shown in Figure 1 together with the Ni II λ1709 and Fe II λ1112 lines. P II λ961 is blended, and the same occurs for P II λ1152 as seen from the EMMI spectrum of Savaglio et al. (1997).

Neutral argon has two strong resonance lines in the ultraviolet region at $\lambda = 1048.220$ and 1066.660 Å. Their oscillator strengths are $f_{1048} = 0.257 \pm 0.013$ and $f_{1066} = 0.064 \pm 0.003$, respectively, from Federman et al. (1992). The whole region of the QSO 0000−2620 spectrum containing the two Ar I lines is shown in Figure 2 to illustrate both the crowding of the Lyα forest and the few windows, which were used for the continuum placing. The Ar lines detected at $z_{abs} = 3.3901$ are zoomed in Figure 3. The data used for Ar result from the sum of only two spectra instead of the whole three, since one of them turned out to be badly contaminated by a cosmic-ray event. The S/N ratio for the

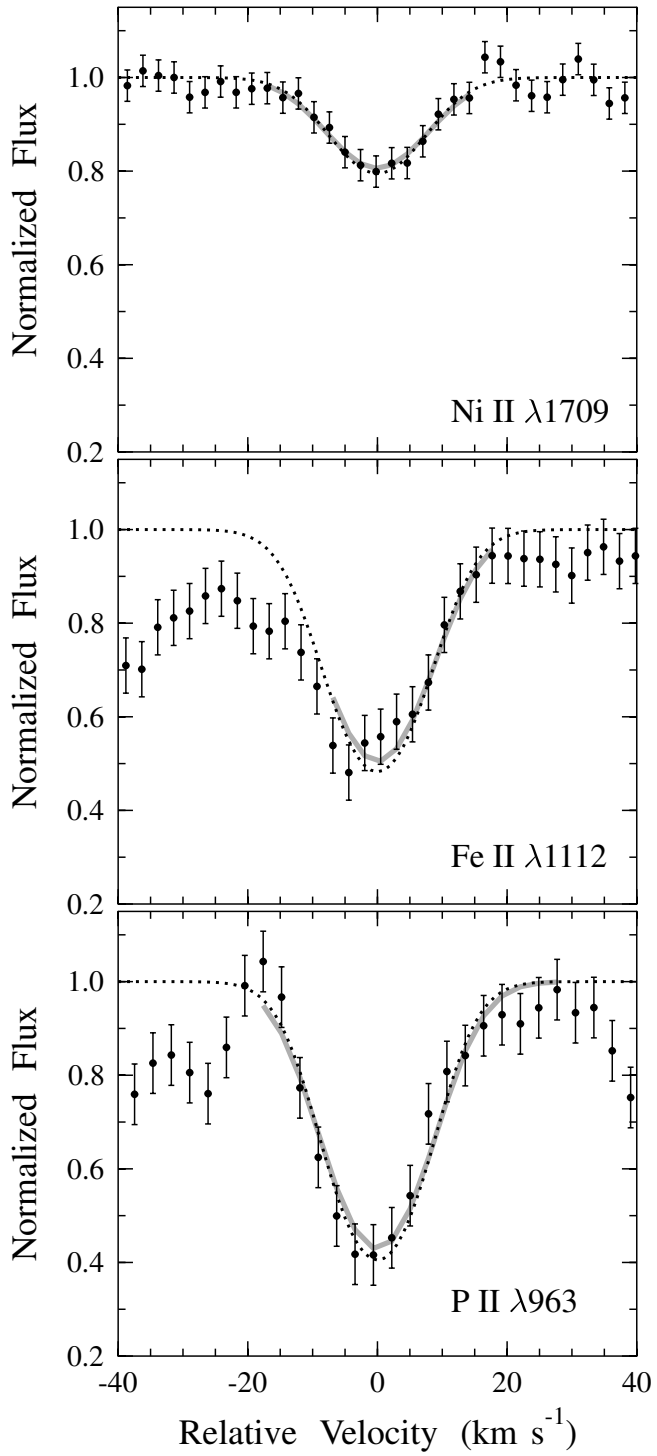

FIG. 1.—Ni II λ1709.600 (*top panel*), Fe II λ1112.048 (*middle panel*), and P II λ963.801 (*bottom panel*) lines associated with the $z_{abs} = 3.3901$ DLA system toward QSO 0000−2620 (*dots and 1 σ error bars*). The lines are aligned taking zero radial velocity in correspondence to $z_{abs} = 3.390127$. Smooth lines are the synthetic spectra obtained from the fit (see text).

[5] $[\text{X/H}] \equiv \log [N(\text{X})/N(\text{H})] - \log [N(\text{X})/N(\text{H})]_{\odot}$.

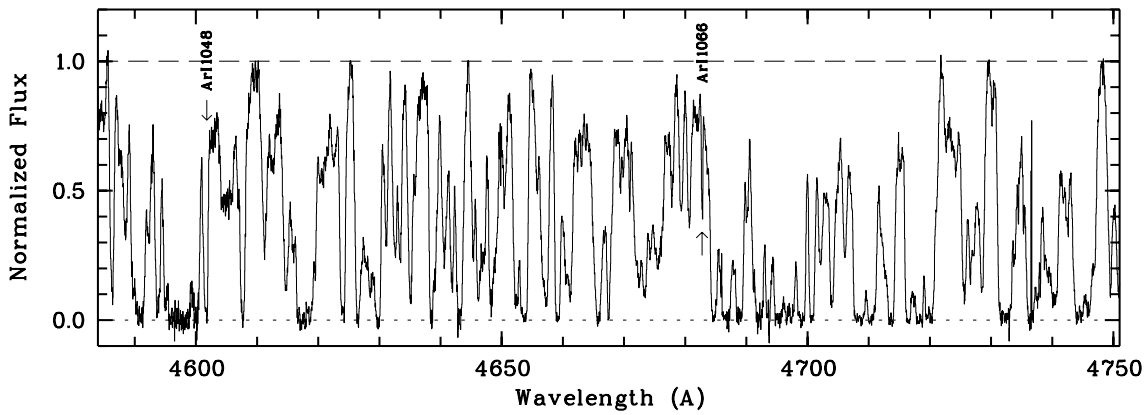

FIG. 2.—A portion of the normalized spectrum of QSO 0000−2620 in the region of the Ar I λ1048.220 and Ar I λ1066.660 lines (λ_{obs} = 4601.8 Å and 4682.8, respectively) associated with the z_{abs} = 3.3901 DLA. All the highest windows in the forest have been used for continuum tracing as well as other windows outside the portion displayed in a spectral range spanning about 1000 Å.

Ar I λ1066 line therefore is 40. As can be seen from the figure, the Ar I λ1066 line is relatively clean, but λ1048 is partly blended with additional absorption. The Ar I line strengths are such that in the Milky Way they tend to be saturated even for tenuous lines of sight, but in our DLA system saturation is not an issue because of the low metallicity, $\bar{Z} \simeq 10^{-2} Z_{\odot}$ (Paper I).

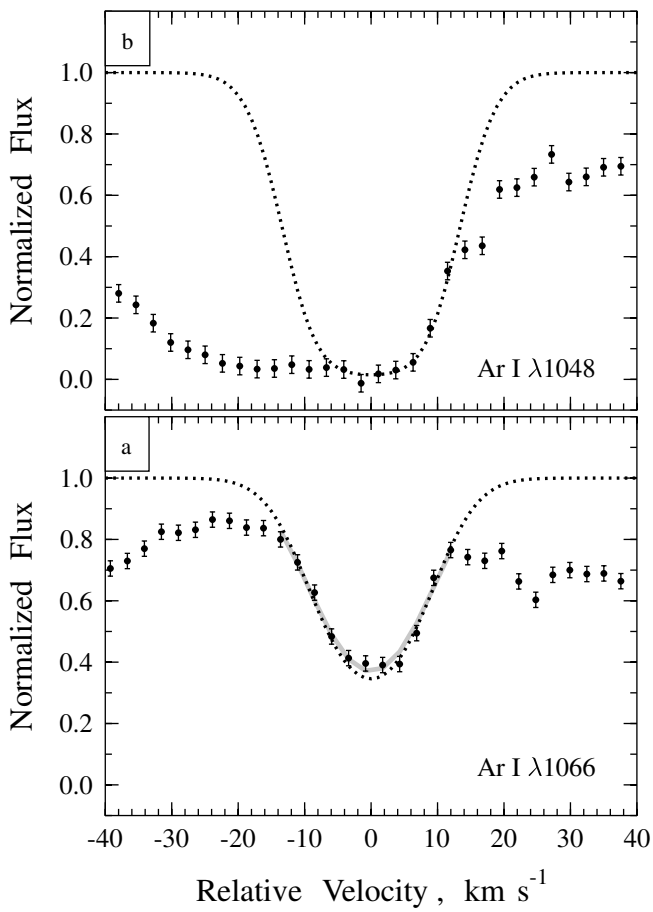

FIG. 3.—(*a*) Ar I λ1066.660 associated with the z_{abs} = 3.3901 DLA system toward QSO 0000−2620 (*dots and error bars*). The line is aligned taking zero radial velocity in correspondence to z_{abs} = 3.390127. Smooth lines are the synthetic spectra obtained from the fit as described in the text. (*b*) A consistent fit of the red wing of the Ar I λ1048.220 (*dotted curve*) based on the best fit of Ar I λ1066 shown in panel *a* by the dotted curve as well.

The measurements of metal absorption lines falling in the Lyα forest have to cope with the possible presence of hydrogen contamination and with a local continuum, drawn by using windows in the Lyα forest which could be located quite far from the feature under analysis.

The P II λ963 line (Fig. 1) shows a rather symmetric profile with its blue side reaching the continuum, while there could be a small contamination in the red wing. The Ar line looks slightly more contaminated with absorption on both sides. The extra absorption around the Ar I line is a continuum-like absorption without signature of discrete features, which makes it hard to model with single H I clouds.

Our previous analysis of both metal and molecular hydrogen lines in this DLA has shown that the line broadening in the z_{abs} = 3.3901 system is mainly caused by macroscopic large-scale, rather than thermal, motions. All absorption lines from H_2 to Zn II show symmetric profiles with the same Doppler parameter of $b \simeq 10$ km s^{-1} within the uncertainty intervals (Papers I and II). The measured broadening parameter, defined as $b = \sqrt{2}\,\sigma_{turb}$, where σ_{turb} is the one-dimensional Gaussian velocity dispersion of ions along the line of sight, gives a turbulent velocity dispersion of about 7 km s^{-1}, a typical value for the Milky Way disk. We can therefore assume that the intrinsic profile of the Ar I λ1066 and P II λ963 lines is the same for all neutral atoms and low-ionized species from the H I region, since they trace the same volume elements.

To calculate the confidence range for the Doppler parameter we make use of all metal lines associated with the DLA redward of the Lyα emission and minimize χ^2 by varying all the other parameters. The calculated χ^2_{min} values as a function of b with the 1 σ and 2 σ confidence levels are shown in Figure 4. At $\chi^2_{min} = 1.148$ the most likely value for b is $10.00^{+0.29}_{-0.25}$ km s^{-1}. The confidence ranges are computed following the procedure described in Press et al. (1992); here we fix the value of b and minimize χ^2 by varying all the other parameters.

The P II λ963 and Ar I λ1066 lines are fitted with a theoretical one-component Voigt profile to the observed intensities together with the full set of six metal lines, for five ionic species, which are located redward of the Lyα emis-

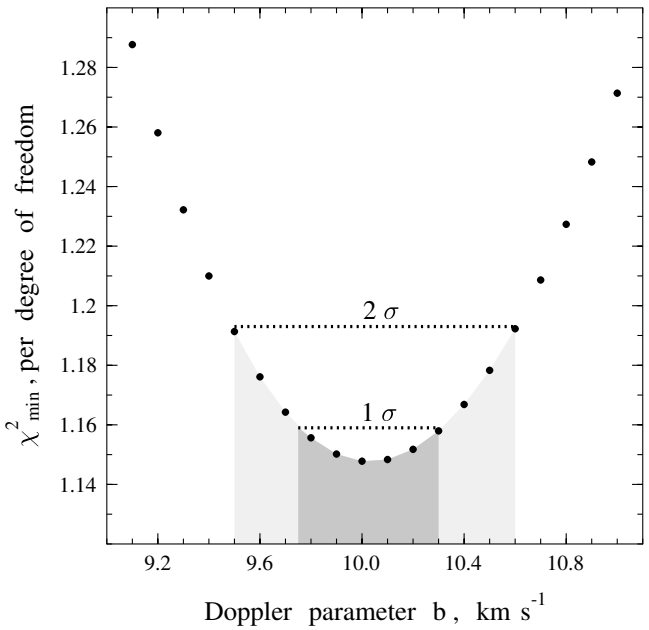

FIG. 4.—Confidence regions in the χ^2_{min}-b plane calculated from the simultaneous fit of the metal absorption lines located redward of the Lyα emission: Fe II λ1611, Ni II λ1709, Si II λ1808, Zn II λ2026, Cr II λ2056, and Cr II λ2062. The parabola vertex corresponds to the best value of $b = 10$ km s^{-1}.

sion, namely, the lines Zn II λ2026.1360, Cr II $\lambda\lambda$2062.2339, 2056.2539, Fe II λ1611.2004, Si II λ1808.0126, and Ni II λ1709.600, assuming that b is the same for all lines and leaving all the elemental column densities as well as the local continuum ($\Delta C/C$) around the P II λ963 and Ar I λ1066 lines free to vary. We have therefore a total of 7 free parameters and 111 and 105 points for P II and Ar I, respectively, thus giving for the former $\nu = 104$ degrees of freedom, and 98 for the latter. All the lines have been previously adjusted in wavelength by using the value of $z_{abs} = 3.390127$, which corresponds to the redshift of the isolated Ni II λ1709 absorption line (Paper I). The calculated theoretical profiles were convolved with a Gaussian instrumental profile with 6 km s^{-1} width.

The best fit for P II gives N(P II) $= 4.29(\pm 0.39) \times 10^{12}$ cm^{-2}, $b = 9.96$ km s^{-1}, and $\Delta C/C = -0.0778$ for a $\chi^2_{min} = 1.10$. The result is shown in Figure 1 by the gray solid curve, whereas points with error bars give the normalized intensities, corresponding to a signal-to-noise ratio $\simeq 15$ pixel^{-1}. Note that the intensities in the bottom panel of Figure 1 are renormalized in concordance with the local $\Delta C/C$. The dotted curve shows the unconvolved theoretical P II profile in the range $|\Delta v| \leq 40$ km s^{-1}. The column densities of Zn, Cr, Si, Ni, and Fe are consistent within 0.02 dex with those found in Paper I. The errors in the P II column density are of 0.04 dex, as can be deduced from Figure 5 (*panel a*), where the χ^2_{min} as a function of the N(P II) column density is shown. The variations for $\Delta C/C$, as well as b, as a function of N(P II) are also shown in panels b and c, respectively. The gray area in panel b marks the range of possible continuum deviations which correspond to the 1 σ confidence interval shown in panel *a*.

The analysis of Ar relies entirely on Ar I λ1066 while Ar I λ1048, of which only a portion is unblended, is checked for consistency with the line model but is not used in the fit. The corresponding signal-to-noise ratio in this spectral

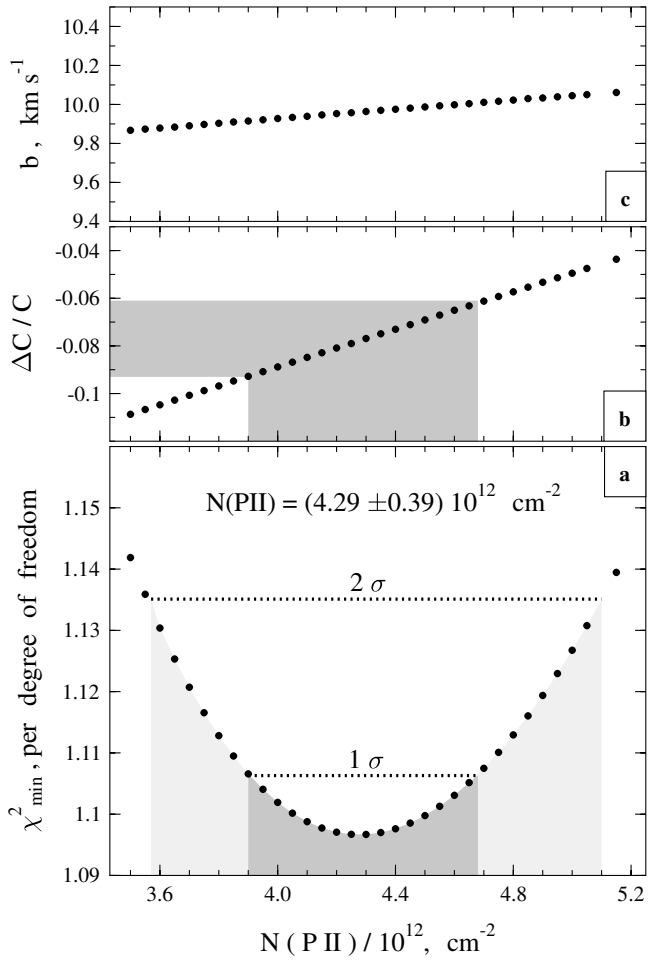

FIG. 5.—Results of the fitting procedure for the P II λ963 line. (*a*) Plot of χ^2_{min} as a function of the column density of the singly ionized phosphorus calculated from the simultaneous fit of P II λ963 and metals Fe II λ1611, Ni II λ1709, Si II λ1808, Zn II λ2026, Cr II λ2056, and Cr II λ2062. The 68.3% and 95.4% confidence levels are marked (*lower and upper horizontal dotted lines*, respectively). The parabola vertex corresponds to the best value of N(P II) $= 4.29 \times 10^{12}$ cm^{-2}. (*b*) The $\Delta C/C$ variations of the local continuum level. The gray area restricts the 1 σ deviations of $\Delta C/C$ in accordance with panel *a*. (*c*) The corresponding values of the Doppler b-parameter.

region is approximately equal to 40. Figure 3 shows the best fit for the one-component profile (*gray continuous curve*) and the intrinsic unconvolved profile for only the Ar I λ1066 line (*dotted curve*). This figure demonstrates that the best fit obtained for Ar I λ1066 provides a consistent fit of the red wing of the stronger Ar I λ1048 line. Note that a decrease of 0.1 dex in the Ar I column density is sufficient to destroy the perfect match present in the Ar I λ1048 line. A $\chi^2_{min} = 1.138$ is found for N(Ar I) $= 1.044(\pm 0.069) \times 10^{14}$ cm^{-2}, $b = 10.05$ km s^{-1} and $\Delta C/C = -0.0086$. Figure 6 shows the confidence levels for the Ar I column density, the variations for $\Delta C/C$, and the Doppler broadening.

To test the whole procedure, we analyzed the Fe II λ1112 line, also shown in Figure 1. This is the only Fe II line in the Lyα forest which is not strongly blended. We then compared the results with those of Fe II λ1611, which is placed redward of the QSO Lyα emission in a clean spectral region and for which a reliable iron column density has already been derived in Paper I. For the Fe II λ1112 line we used the empirical oscillator strength ($f_{1112} = 0.0062$) derived recently by Howk et al. (2000) by means of *FUSE* obser-

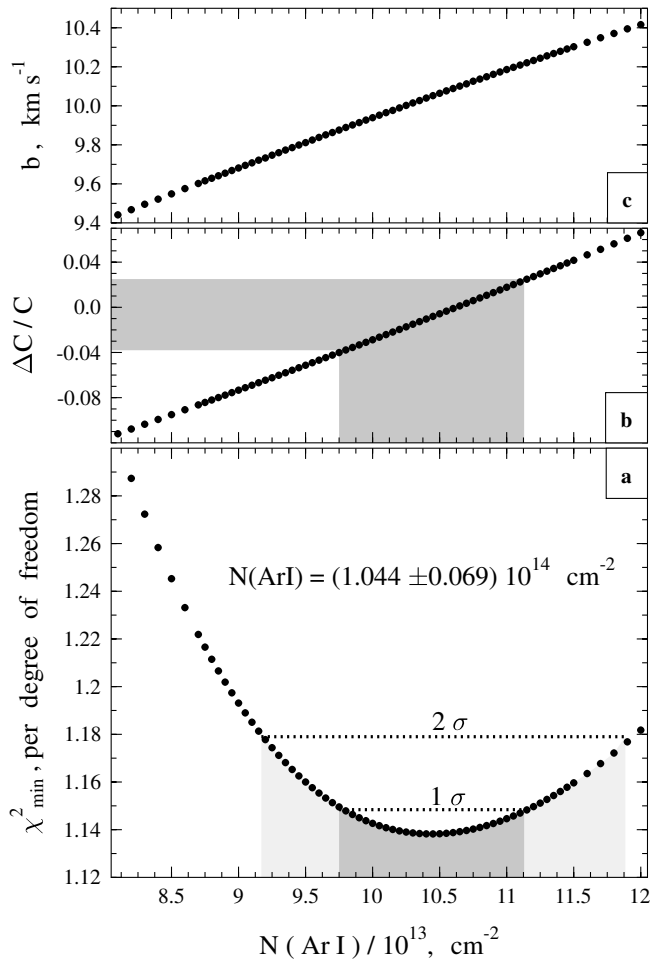

FIG. 6.—As in Fig. 5, but for the Ar I λ1066 line. The parabola vertex in panel *a* corresponds to the best value of $N(\mathrm{Ar\ I}) = 1.044 \times 10^{14}\ \mathrm{cm}^{-2}$.

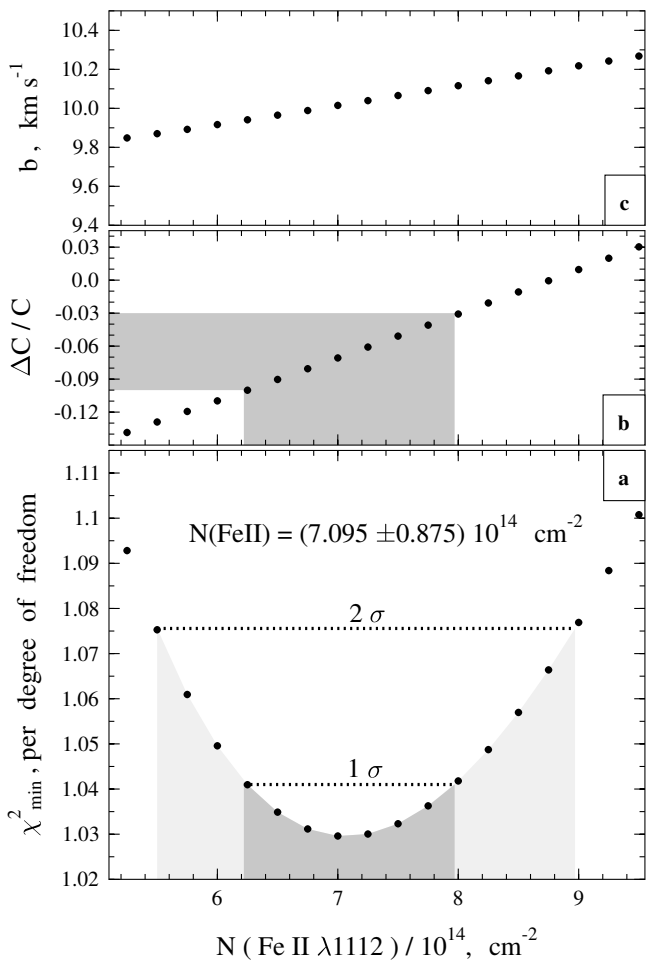

FIG. 7.—As in Fig. 5, but for Fe II λ1112 and the following set of the metal absorption lines from the red portion of the quasar spectrum: Ni II λ1709, Si II λ1808, Zn II λ2026, Cr II λ2056, Cr II λ2062. The parabola vertex in panel *a* corresponds to the best value of $N(\mathrm{Fe\ II}\ \lambda1112) = 7.095 \times 10^{14}\ \mathrm{cm}^{-2}$.

vations. A $\chi^2_{\min} = 1.0299$ is found for $N(\mathrm{Fe\ II}) = 7.095(\pm0.875) \times 10^{14}\ \mathrm{cm}^{-2}$, $b = 10.07\ \mathrm{km\ s}^{-1}$, and $\Delta C/C = -0.066$. In this case we used only six metal lines from the red part of the quasar spectrum excluding Fe II λ1611 from the χ^2-minimization procedure. Thus we had 6 free parameters, $N_{\mathrm{Ni\ II}}$, $N_{\mathrm{Si\ II}}$, $N_{\mathrm{Zn\ II}}$, $N_{\mathrm{Cr\ II}}$, b, $\Delta C/C$, 93 data points, and $\nu = 87$ degrees of freedom, and calculated $\chi^2_{\min}$ as a function of N(Fe II λ1112). The calculated confidence intervals are shown in Figure 7. The mean iron column density for Fe II λ1112 is 0.02 dex lower than that derived from Fe II λ1611 in Paper I and is fully consistent within errors. This shows that we can indeed recover the ion column density accurately even though the line is falling in the Lyα forest with random Lyα interlopers and uncertainties associated with the continuum drawing. The derived column densities and abundances for Ar and P, together with those obtained for other species in previous studies, are reported in Table 1.

The results presented above differ quite slightly from those obtained from a more commonly used analysis in which the continuum is kept fixed while both the broadening and the column density are left free to vary. In this approach we obtain for phosphorus $N(\mathrm{P\ II}) = 10^{12.70\pm0.04}\ \mathrm{cm}^{-2}$ and $b = 10.3^{+1.4}_{-1.1}\ \mathrm{km\ s}^{-1}$, while for argon $N(\mathrm{Ar\ I}) = 10^{14.02\pm0.02}\ \mathrm{cm}^{-2}$ and $b = 9.95 \pm 1\ \mathrm{km\ s}^{-1}$ when the P II λ963 and Ar I λ1066 lines were analyzed separately. The shift of the P II line is $\Delta v = -0.01\ \mathrm{km\ s}^{-1}$, and that of the Ar I line center is, namely, $\Delta v = -0.66\ \mathrm{km\ s}^{-1}$, which is less than one-half of the pixel width.

The fact that both lines have the same centers and the same *b*-parameters, which are very similar to those of metal lines observed in the low line density portion of the spectrum redward of the Lyα emission line, shows that the contamination of Ar I and P II lines observed in the Lyα forest is not significant in the $z_{\mathrm{abs}} = 3.3901$ system toward QSO 0000−2620.

2. DISCUSSION

For both argon and phosphorus there are no determinations of the intrinsic abundances in either dwarf or giant stars because argon has optical transitions from very high excitation levels, and phosphorus shows too faint lines in stellar spectra. P was measured in chemically peculiar stars (Castelli et al. 1997), halo horizontal-branch stars by Bonifacio et al. (1995), and sdB by Ohl et al. (2000). However, the elemental abundances in these stars are likely modified by atmospheric processes such as diffusion. A firm identification of the P IV and P V has been made by Junkkarinen et al. (1997) in the BAL QSO PG 0946+301, and a remarkable overabundance of phosphorus with $\mathrm{P/C} \approx 60(\mathrm{P/C})_{\odot}$ was found.

TABLE 1

COLUMN DENSITIES AND ABUNDANCES IN THE DUST-FREE PATTERN AT $z_{abs} = 3.3901$

Element	log (N)[a]	$(X/H)_{DLA}$	$(X/H)_{\odot}$[b]	[X/H][c]
$^{1}_{1}$H	21.41 ± 0.08[d]	...	...	...
$^{14}_{7}$N	14.73 ± 0.02[g]	-6.68 ± 0.083	-4.03 ± 0.07	-2.65 ± 0.12[e]
$^{16}_{8}$O	16.42 ± 0.10[g]	-4.99 ± 0.128	-3.13 ± 0.07	-1.86 ± 0.15[e]
$^{28}_{14}$Si	15.06 ± 0.02	-6.35 ± 0.083	-4.44 ± 0.01	-1.91 ± 0.08[e]
$^{31}_{15}$P	12.63 ± 0.04	-8.78 ± 0.089	-6.47 ± 0.04	-2.31 ± 0.10[f]
$^{32}_{16}$S	14.70 ± 0.03	-6.71 ± 0.085	-4.80 ± 0.01	-1.98 ± 0.09[d]
$^{36}_{18}$Ar	14.02 ± 0.03	-7.39 ± 0.085	-5.48 ± 0.04	-1.91 ± 0.09[f]
$^{52}_{24}$Cr	13.10 ± 0.03[g]	-8.31 ± 0.085	-6.32 ± 0.03	-1.99 ± 0.09[e]
$^{56}_{26}$Fe	14.87 ± 0.03	-6.54 ± 0.085	-4.50 ± 0.01	-2.04 ± 0.09[e]
$^{58}_{28}$Ni	13.39 ± 0.03	-8.02 ± 0.085	-5.75 ± 0.01	-2.27 ± 0.09[e]
$^{64}_{30}$Zn	12.01 ± 0.05	-9.40 ± 0.094	-7.33 ± 0.04	-2.07 ± 0.10 [e]

[a] N in cm^{-2}.
[b] Data from Grevesse et al. 1996 except for Ar where the weighted average values from Sofia & Jenkins 1998 are used.
[c] Errors in [X/H] include errors in column densities and in solar abundances.
[d] From Lu et al. 1996.
[e] From Molaro et al. 2000.
[f] This work.
[g] Mean values.

The lack of such important observational reference complicates the interpretation of the Ar and P abundances in the DLA systems. Nevertheless, we may compare the measured [Ar/H] and [P/H] ratios with theoretical predictions based on integrating massive star yields over an initial mass function given (IMF), for instance, by Timmes et al. (1995, hereafter TWW). In this section we consider such issue, and other physical properties of the $z_{abs} = 3.3901$ system.

2.1. *Argon Abundance*

2.1.1. *Local Stellar Ionization*

Argon is an extremely volatile element. It has been detected and studied in the Galactic ISM by means of *Copernicus*, Interstellar Medium Absorption Profile Spectrograph (IMAPS), and recently by *FUSE*. The gas-phase (Ar/H) ratio in the Galactic interstellar medium is found to be below its solar value with reduction factors varying with the lines of sight. Fitzpatrick (1996) argued that abundances of undepleted elements in the ISM such as C, N, and O are below their solar values, but this cannot explain the line-of-sight variations and the considerable amount of the observed Ar deficiency, $[Ar/H] \lesssim -0.5$ dex. Since Ar can be hardly depleted into dust grains, Sofia & Jenkins (1998) suggested that the apparent Ar deficiency is caused by a partial ionization of Ar by nearby UV stellar radiation.

Ar I has an extraordinarily high photoionization cross section for photons with energy higher than the IP = 15.76 eV. Its photoionization cross section is about 10 times higher than that of H I over a broad range of energies. Therefore, for a cloud that is not thick enough to shield its interior from outside sources of ionizing radiation, the UV photons may penetrate the cloud and partially ionize hydrogen, argon, and other elements. In this case the fraction of Ar I can be lower than the corresponding fraction of H I, since the absorption cross section of hydrogen diminishes in proportion to ν^3 for energies $h\nu > 13.6$ eV, an effect which may lead to an apparent deficiency of argon with respect to hydrogen if one assumes that both elements are mostly neutral.

Reversing the argument presented by Sofia & Jenkins on the Ar I deficiency in the local interstellar medium, the coincidence of the Ar abundance with those of O, Si, and S (see Table 1) implies the absence of significant photoionizing flux from stars along the line of sight throughout the $z_{abs} = 3.3901$ damped galaxy. Otherwise, the presence of stellar photons with $h\nu > 13.6$ eV would decrease the Ar I abundance. The same effect is not observable in O I, although neutral oxygen also has a photoionization cross section larger than that of H I. Oxygen ionization fractions are coupled with those of hydrogen via resonant charge exchange reactions. Therefore, there is observational evidence that in this particular damped system the observed ionic species are from their dominant ionization stages in the H I gas and, hence, their abundances do not require ionization corrections which may be caused by a hard radiation field in a uniform and fluctuating gas density absorbing region, respectively (Viegas 1995; Levshakov et al. 2000a). We would like to emphasize once more that our measurement of Ar I rules out the presence of active star formation regions and of significant partly ionized gas along the line of sight at $z_{abs} = 3.3901$.

Steidel & Hamilton (1992) identified a galaxy at 2.″8 from the QSO 0000−2620 sight line, which was supposed to be responsible for the $z_{abs} = 3.3901$ damped system. Giavalisco et al. (1994) found no Lyα flux in correspondence of this object by means of narrow band imaging placing a 3 σ upper limit of 1.2×10^{-17} ergs s^{-1} cm^{-2}. The object identified in Steidel & Hamilton (1992) is probably a high-redshift galaxy at $z \sim 2.8$ (C. C. Steidel 2000, private communication), and therefore the galaxy at $z = 3.39$ still remains undetected. However, the upper limit provided by Giavalisco et al. (1994) in the Lyα emission refers to the sky area around the QSO and remains valid regardless of the nature of the DLA candidate. The general lack of Lyα emission from DLA systems has been commonly explained by the effect of dust and resonant scattering which can attenuate Lyα photons (Charlot & Fall 1991, 1993). However, the extremely low dust content in our system with a dust-to-gas ratio of less than 10^{-3} of the Milky Way value, coupled with no detectable effects on the Ar I abundance, suggests

that most likely the DLA system in question is not a site of intense star formation.

2.1.2. *A Universal IMF*

Observations of emission lines in ionized H II regions of spiral and irregular galaxies provide abundances for O, S, and Ar among the others. None of these elements is expected to be heavily depleted into the solid phase as dust (Savage & Sembach 1996). It has already been pointed out that the abundance ratios [S/O] and [Ar/O] appear to be universally constant and independent of metallicity over about 2 decades of oxygen abundances (e.g., Henry & Worthey 1999). Since O production depends on the progenitor mass while Ar and S do not, the implication of this constant ratio is that either the initial mass function is universally constant or that the observed elemental ratios are not sensitive to IMF variations.

Sulfur and argon originate from explosive oxygen burning in Type II supernova events through the chain $^{16}O + {}^{16}O \rightarrow {}^{28}Si + {}^{4}He$, then $^{28}Si + {}^{4}He \rightarrow {}^{32}S$, and $^{32}S + {}^{4}He \rightarrow {}^{36}Ar$. However, substantial amounts of S and Ar may be manufactured in Type Ia supernova events (Nomoto et al. 1997). Considering the values of Izotov & Thuan (1999) for the extragalactic H II metal-poor regions, we have $\log(S/O) = -1.55 \pm 0.06$ (rms) and $\log(Ar/O) = -2.25 \pm 0.09$ (rms). Similar results, $\log(S/O) = -1.48 \pm 0.06$ (rms) and $\log(Ar/O) = -2.32 \pm 0.05$ (rms), for the same class of objects have been recently obtained by Kniazev et al. (2000).

These observed ratios are comparable to the theoretical predictions of Woosley & Weaver (1995), Nomoto et al. (1997), and Samland (1998) in which $\log(S/O) \approx -1.75$, -1.9, -1.6, and $\log(Ar/O) \approx -2.45$, -2.7, and -2.4, respectively. The theoretical predictions fall somewhat below the observed range, and either an overproduction of O in the models or a significant production of S and Ar in Type Ia supernovae are advocated.

Our results listed in Table 1 show that the Ar abundance follows closely the other α-chain element abundances in the $z_{abs} = 3.3901$ system. The absolute oxygen abundance in this DLA is $\log(O/H) + 12 \approx 7$, i.e., 1 order of magnitude below the value obtained in the most metal-poor galaxies where these elements were measured. The measured log (S/O) and log (Ar/O) ratios are -1.72 ± 0.15 and -2.40 ± 0.15, respectively, i.e., very close to the observed ratio in blue compact and spiral galaxies. This strongly favors the universality of (S/O) and (Ar/O) ratios. The implication pointed out by Henry & Worthey (1999) that either the IMF is universally constant or the stellar mass range which produces these elements is narrow enough to make the ratios insensitive to IMF variations is reinforced and further extended to much more deficient material detected at $z_{abs} = 3.3901$.

2.1.3. α-*Capture versus* Fe-*Peak Element Ratios*

Most α-particle nuclei are synthesized primarily by Type II supernovae during the early stages of the galaxy chemical evolution, while the Fe-group elements are primarily produced by Type Ia supernovae and build up over longer timescales. As a result, in the early phases of chemical enrichment the α-chain elements are expected to be relatively more abundant than the iron-peak elements.

Argon is a typical product of Type II SNe, and like zinc it is not depleted in the interstellar medium. This makes the [Ar/Zn] ratio a new and interesting dust-free diagnostic tool for verifying the presence of the α-chain element enhancement. By combining the present abundances with those previously determined (see Table 1), we have at our disposal a set of four indicators for the α-chain element abundances such as O, Si, S, Ar, and four indicators for the abundances of iron-peak elements such as Cr, Fe, Ni, and Zn. This is a close to unique circumstance among the DLA systems studied so far.

The measured [O, Si, S, Ar/Cr, Fe, Ni, Zn] ratios reported in Table 2 for quantitative comparison provide $\langle$[α-chain/iron-peak]$\rangle = 0.20 \pm 0.03$ dex (the weighted mean and dispersion) which becomes 0.12 ± 0.02 when the slightly deviating Ni is not considered. In the case that Ni turned out to be a better Fe-peak indicator than Fe, Cr, and Zn, we would indeed find that [O, Si, S, Ar/Ni] are $+0.41$, $+0.36$, $+0.36$, and $+0.36$, respectively. However, Prochaska & Wolfe (1999) measured Ni II λ1751.910 and found $[Ni/H] = -2.335 \pm 0.085$, which becomes $[Ni/H] = -1.952 \pm 0.085$ when the log *gf* values are taken from Fedchak & Lawler (1999), as we did for Ni II λ1709.600 (Paper I). The slightly different abundance obtained from the two Ni II lines prevents Ni from being considered a safe proxy to the iron-peak abundances.

An [alpha/iron-peak] ratio of ≈ 0.1 is significantly lower than similar quantity in Galactic stars with comparable metallicities, [O, Si, S/Fe] $\simeq$ 0.3–0.6 dex (McWilliam 1997 and references therein). The difference would be even more striking if the high O values of [O/Fe] = 0.7 found in halo stars at [Fe/H] = −2 by Israelian et al. (1998) and Boesgaard et al. (1999) were confirmed. Implications of low α-chain/iron-peak element ratios are discussed in Paper I, and the reader is referred to it for additional details. Here we notice that the lack of significant [Ar/Zn] enhancement corroborates our previous results on this system as well as the assumption that, on the basis of their relative element abundances, at least some of the DLA galaxies seem to undergo a chemical evolution which differs from that of the Milky Way (Centurión et al. 2000). An analysis of the zinc abundances in the thick disk stars by Prochaska et al. (2000) showed that zinc could be mildly overabundant with respect to iron with $[Zn/Fe] = 0.09 \pm 0.023$, a slight difference from the thin disk and halo behavior found by Sneden et al. (1991). However, in our DLA system $[Zn/Fe] = -0.03 \pm 0.06$ and $[Zn/Cr] = -0.08 \pm 0.06$, which suggests that in the DLAs zinc tracks Fe and Cr closely.

2.2. *Phosphorus Abundance*

Phosphorus is likely a nondepleted element. Dufton et al. (1986) and Jenkins et al. (1986) found that phosphorus is essentially undepleted along sight lines sampling low-density neutral gas and is depleted by approximately 0.5 dex in cold clouds. However, P is found strongly depleted in dense star-forming molecular clouds (Turner et al. 1990). From *FUSE* observations, Friedman et al. (2000) obtained $[Fe/P] \approx -0.6$ and -0.7 for the Milky Way and LMC

TABLE 2

THE [O, SI, S, AR/CR, FE, NI, ZN] RATIOS IN THE $z_{abs} = 3.3901$ SYSTEM

	Cr	Fe	Ni	Zn
O	0.13 ± 0.13	0.18 ± 0.13	0.41 ± 0.13	0.21 ± 0.14
Si	0.08 ± 0.05	0.13 ± 0.07	0.36 ± 0.04	0.16 ± 0.05
S	0.08 ± 0.05	0.13 ± 0.04	0.36 ± 0.04	0.16 ± 0.07
Ar.....	0.08 ± 0.07	0.13 ± 0.06	0.36 ± 0.06	0.16 ± 0.08

diffuse interstellar clouds, respectively, and argued for a significant incorporation of iron into dust grains in both galaxies. The phosphorus abundance provided here is one of the few available for this element in any astronomical site and the only one in little-processed material.

In our DLA the abundances of the refractory elements Fe and Cr are close to that of the nonrefractory element Zn, showing the absence of significant dust concentration along the line of sight (Paper I). Such a circumstance is extremely rare among DLAs, since even in the cases with low element depletion considered by Pettini et al. (2000), a difference between Zn and Fe, Cr and Ni has been always observed, with the exception of the damped system toward QSO 0454+039 where [Zn/Cr] ≈ 0 within the errors. Moreover, the extremely low fraction of molecular hydrogen $f(H_2) \equiv 2N(H_2)/N(H)_{total} \simeq 4 \times 10^{-8}$ in our DLA (Paper II) rules out a significant depletion of P in a variety of molecular compounds. Taking into account that the absorbing gas is mostly neutral, as discussed above, we conclude that the observed gas-phase P abundance reflects the total amount of P.

The low abundance of P is close to those of other elements (see Table 1) and supports independently the early suggestion that the $z_{abs} = 3.3901$ galaxy has indeed a low metallicity. In the context of the other published data this result suggests a possible mild decrease in the damped abundances at high redshift, which, however, is not evident when the column density–weighted mean is considered (Prochaska & Wolfe 2000; Vladilo et al. 2000).

Theoretically the processes that produce the odd-Z element phosphorus in late stages of stellar evolution are not identified clearly. As Burbidge (1999) pointed out, the P synthesis was virtually ignored by Burbidge et al. (1957). The only stable isotope is ^{31}P, which is strongly underproduced in the explosive O burning. P is likely produced in the carbon and neon shell burning by neutron capture, similarly to the parent nuclei ^{29}Si and ^{30}Si. No significant P production is found during the explosion phases (Woosley & Weaver 1995).

Phosphorus abundance, like that of the other odd-Z elements Na and Al, should be proportional to η, the total neutron excess in a given amount of matter,[6] which is $\eta \approx 1.5 \times 10^{-3}(\zeta/\zeta_\odot)$, where $\zeta_\odot \approx 0.02$ denotes the fraction by mass of matter composed of nuclei with atomic number $Z \geq 6$ (Arnett 1971, 1996). As the metallicities decrease, the available nuclei which provide the neutron excess decrease too. However, in the primordial stellar yields Arnett (1996) found that the odd-Z nuclei are underabundant with reference to the even-Z neighbors, but the effect is much smaller than that predicted by simple arguments of linear increase of neutron excess with metallicity. Theoretical models by Woosley & Weaver (1995) lead also to substantial P production with P yields showing a metallicity dependence which is more pronounced at very low metallicities.

In our DLA the measured ratios [P/Si] $= -0.40 \pm 0.13$ and [P/S] $= -0.40 \pm 0.13$ provide evidence for a mild odd-even effect, which, however, is less than what is expected on the basis of the Woosley & Weaver (1995) and Limongi et al. (2000) yields. A similar value for [P/S] $= -0.34 \pm 0.07$ has been derived by Outram et al. (1999) in the DLA at $z_{abs} = 2.625$ toward GB 1759+7539, which with [Fe/H] $= -1.31$ is, however, somewhat more metal rich than the DLA studied here.

In stellar spectroscopy the element abundances are traditionally discussed as related to iron, [X/Fe], and as a function of the iron-to-hydrogen ratio, [Fe/H]. Following this way, in Figure 8 we compare our results with theoretical predictions, since in our case there is no significant dust depletion in the $z_{abs} = 3.3901$ absorber and, hence, [Fe/H] can be used as a reference ratio. Figure 8 shows the result of such comparison between the elements listed in Table 1 (dots with 3 σ error bars) and the theoretical prediction (*shaded area*). The width of the shaded area just above a marked element shows the uncertainty range (± 0.2 dex) for the relative abundance of this element [X/Fe] at fixed metallicity [Fe/H] $= -2.0$. The uncertainty of theoretical predictions is caused by unknown model parameters as described in TWW. The upper limit for the nitrogen-to-iron ratio is set by calculations which include enhanced convection prescriptions, but the lower limit is not defined at low metallicities, since the standard TWW set of massive stars does not produce significant nitrogen yields. We see from Figure 8 that there exists a general consistency between the observed [X/Fe] ratios and the theoretical predictions. The P abundance is slightly suppressed, whereas Ar behaves like other α-chain elements. However, the same consistency is not found if compared with the halo stellar abundance pattern, where α-chain elements are much more enhanced. There are intrinsic uncertainties in the $M \geq 30\ M_\odot$ extremely metal-poor massive-star models, which may be important here. TWW suggest that their Fe yields may be overestimated by a factor of 2, which, if applied in Figure 8, would shift all abundances by 0.3 dex along the ordinates. For instance in the Samland (1998) analysis the α-chain elements are more enhanced in agreement with what is observed in the Galactic halo stars.

The P abundance found in our DLA is slightly lower than Fe and the other iron-peak elements, showing that P was slightly undersolar at low metallicities. Since P is produced almost entirely by massive stars to achieve the higher

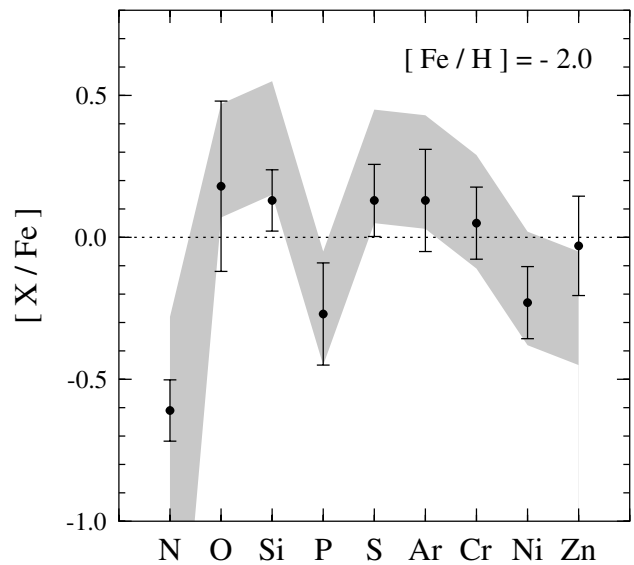

FIG. 8.—Theoretical nucleosynthetic yields (the shaded area shows ± 0.2 dex uncertainty range; see text for more details) for the metallicity [Fe/H] $= -2.0$ in the standard model of the galactic chemical evolution by Timmes et al. (1995). The dots with 3 σ error bars mark the measured relative abundances [X/Fe] at $z_{abs} = 3.3901$ toward QSO 0000−2620.

[6] The neutron excess is defined as $\eta = (n_n - n_p)/(n_n + n_p)$, where n_n represents the total number of neutrons per gram, both free and bound in nuclei, and n_p the corresponding number for protons (Arnett 1971).

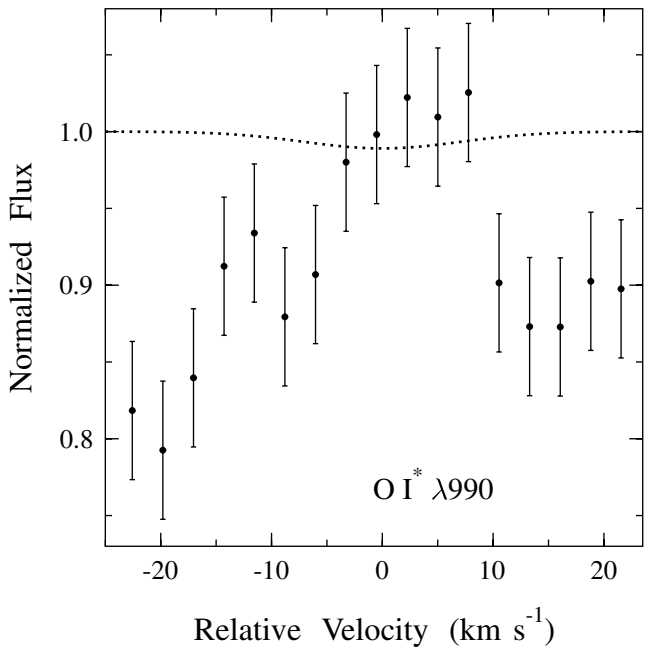

FIG. 9.—O I* λ990.2043 (transition $^3P_1 \rightarrow {}^3D_2$) expected position in the $z_{abs} = 3.3901$ DLA system toward QSO 0000−2620. The radial velocity scale is the same as in Figs. 1 and 3. The dotted curve is then convolved with the spectrograph function synthetic spectrum constraining the total O I* column density for the fixed value of $b = 10$ km s^{-1}.

solar value, its production must increase with the metallicity of the gas also to compensate the contribution to iron made by Type Ia SNe. In other words the P yields have to be necessarily metallicity dependent. This illustrates well how direct P observations in metal-poor environments can be used to constrain the parameter values in the stellar nucleosynthesis theory.

The obtained results on P and Fe abundances do not seem to agree with the dust formation processes in the Galaxy where iron depletion in the diffuse interstellar clouds has been well studied. In § 1, two possible mechanisms of the dust formation processes were outlined, and it was noted that P and Fe abundances may be used for choosing one of them. For instance, if the dust grains grow in the interstellar medium we could detect a disparity in P and Fe gas-phase abundances as seen in the Galactic diffuse clouds. Obviously this is not the case for the $z_{abs} = 3.3901$ system. If, however, the dust grains are formed in hot shells of supernova remnants—an example of this process has recently been presented by Arendt et al. (1999), who revealed Fe protosilicate in the Cas A ejecta—then we should observe a gas-phase depletion for both P and Fe, since they have the same condensation temperature. This has not been found in our DLA system either. Therefore, neither of the two possible mechanisms of dust formation seem to work in the $z_{abs} = 3.3901$ damped Lyα cloud. Taking into account that both volatile and nonvolatile elements do not show significant differences in their abundances from the expected quantities, we may conclude that in this DLA system possible destructive processes are also insufficient to cause some evaporation of the volatile substances.

2.3. *Neutral Hydrogen Density*

The number density of neutral hydrogen, n_{HI}, in the $z_{abs} = 3.3901$ system can be estimated by using the relative population ratio of the first excited state O I* ($^3P_1$) to the ground state O I ($^3P_2$).

In H I regions with temperatures ranging from 100 to 1000 K, the rate coefficients for collisions with hydrogen atoms are larger than those for electron collisions when the electron density, n_e, is small, i.e., $n_e/n_{H\,I} \lesssim 10^{-2}$ (Bahcall & Wolf 1968). If we also neglect the contributions of proton and molecular hydrogen collisions, the equilibrium equation for the three-level system ($^3P_2$, $^3P_1$, and $^3P_0$ states of O I) can be written as

$$\frac{N(\text{O I*})}{N(\text{O I})} \simeq \frac{n_H(k_{01} + k_{02})}{A_{10}}, \quad (1)$$

where k_{01} and k_{02} are the rate coefficients of the O-H collisions, and $A_{10} = 8.95 \times 10^{-5}$ s^{-1} is the spontaneous transition probability (all other collisional and photon rates are negligibly small in this case).

The rate coefficients for the downward transitions k_{10} and k_{20}, induced by O-H collisions in the temperature range from 50 to 1000 K, are given by Launay & Roueff (1977). The corresponding excitation rates for upward transitions can be calculated from the principle of detailed balance, which implies

$$k_{0i} = \frac{g_i}{g_0} \exp\left(-\frac{\Delta E_{0i}}{T}\right) k_{i0}, \quad (2)$$

where $g_2 = 1$, $g_1 = 3$, and $g_0 = 5$ are the degeneracies of states $^3P_0$, $^3P_1$ and $^3P_2$, respectively. $\Delta E_{01} = 228$ K and $\Delta E_{02} = 326$ K are the energy differences between the ground state and the corresponding fine-structure levels.

In the observed spectrum of QSO 0000−2620 the most stringent limit on the population of the $^3P_1$ state may be set by the O I* λ990.2043 transition (see Fig. 9). Using the b-parameter value of 10 km s^{-1}, we estimate N(O I*) $\leq 1.9 \times 10^{12}$ cm^{-2}, at 1 σ confidence level. Then, with the observed ratio N(O I*)/N(O I) $\leq 7.2 \times 10^{-5}$, and assuming $T \simeq 10^3$ K (see Paper II), we find from Launay & Roueff $k_{10} = 9.22 \times 10^{-11}$ cm^3 s^{-1} and $k_{20} = 3.80 \times 10^{-11}$ cm^3 s^{-1} or $k_{01} = 4.4 \times 10^{-11}$ cm^3 s^{-1} and $k_{02} = 0.55 \times 10^{-11}$ cm^3 s^{-1}, and get $n_{HI} < 130$ cm^{-3}. (Note that for the chosen temperature and for $n_e/n_{H\,I} = 10^{-2}$ the rate coefficient for collisions with electrons is equal to 3×10^{-12} cm^3 s^{-1} if the collision strength is $\Omega_{01} = 3.35 \times 10^{-3}$, according to Bell et al. 1998.)

Since O I* traces neutral phase regions along the line of sight, the above result may be considered as the upper limit for the whole H I cloud. If this is the case, then the physical size of the $z_{abs} = 3.3901$ cloud is $L > 7$ pc. If the lower limit is $n_{H\,I} > 1$ cm^{-3}, which is typical for the Galactic diffuse H I clouds, then $L < 850$ pc. Comparable sizes have also been placed by Giardino & Favata (2000) for the second damped system at $z_{abs} = 3.054$ toward QSO 0000−2620 from the detection of the C II and C II* absorptions.

3. CONCLUSIONS

UVES observations of the quasar QSO 0000−2620 gave as a result the first detection of the Ar I λ1066.660 and P II λ963.801 transitions that originated in the damped Lyα system at $z_{abs} = 3.3901$. The derived abundances are [Ar/H] $= -1.91 \pm 0.09$ and [P/H] $= -2.31 \pm 0.10$, with most errors originating in the neutral hydrogen column density.

The phosphorus abundance provided here is one of the few available for this element in any astronomical site and

unique in material poor of metals. The low abundance of the nonrefractory element P confirms the low metallicity level of the galaxy, which is therefore in the early stages of its chemical evolution. The P abundance is slightly below the iron-peak elements and, when compared to its close nuclei S and Si, P shows mild evidence of an odd-even effect, but less extreme than that predicted by theoretical models by Woosley & Weaver (1995) or Limongi et al. (2000).

Ar abundance is remarkably similar to that of oxygen, sulfur, and silicon, [O/H] $= -1.86 \pm 0.15$, [S/H] $- 1.98 \pm 0.09$, and [Si/H] $= -1.91 \pm 0.08$. Ar has a large photoionization cross section, and the similarity of its abundance with the other α-chain elements implies the absence of significant photoionization either by external or internal sources.

The log (Ar/O) and log (Ar/S) ratios are almost the same as those found in the blue compact galaxies and in present-day galaxies where O is more abundant by one or two orders of magnitude. This strengthens the constancy of Ar/O and Ar/S ratios and lends support to the existence of a universal IMF.

In the DLA under study the relative abundances of α-chain and iron-peak elements, as measured by an unprecedented number of indicators, show only a mild overabundance at variance with the pattern of the old stellar population of the Galaxy. Since this DLA is a dust-free system, its chemical composition and the relative abundances of the observed species may be used to constrain model parameters in the theoretical calculations of stellar nucleosynthesis in the metal-poor gas.

Measurements of the volatile and nonvolatile element abundances have shown that none of the known processes of dust formation or destruction is effective in the $z_{\rm abs} = 3.3901$ galaxy.

Finally, the upper limit to the population of the first fine-structure level in the ground state of O I is used to infer a lower limit to the physical dimension of the DLA system, which is placed at $L > 7$ pc.

The high-resolution spectra analyzed in this paper are of unique quality and were obtained during the first nights of commissioning of a new instrument at a new telescope. For these results we are indebted to all ESO staff involved in the VLT construction and in UVES commissioning. We thank also the referee Jason X. Prochaska for his useful comments and remarks. The work of S. A. L. is supported by RFBR grant 00-02-16007.

REFERENCES

Arendt, R. G., Dwek, E., & Moseley, S. H. 1999, ApJ, 521, 234
Arnett, W. D. 1971, ApJ, 166, 153
———. 1996, Supernovae and Nucleosynthesis (Princeton: Princeton Univ. Press)
Bahcall, J. N., & Wolf, R. A. 1968, ApJ, 152, 701
Bell, K. L., Berrington, K. A., & Thomas, M. R. J. 1998, MNRAS, 293, L83
Boesgaard, A. M., King, J. R., Deliyannis, C. P., & Vogt, S. S. 1999, AJ, 117, 492
Bonifacio, P., Castelli, F., & Hack, M. 1995, A&AS, 110, 441
Burbidge, E. M. 1999, Ap&SS, 265, 99
Burbidge, E. M., Burbidge, G. R., Fowler, W. A., & Hoyle, F. 1957, Rev. Mod. Phys., 29, 547
Castelli, F., Parthasarathy, M., & Hack, M. 1997, A&A, 321, 254
Centurión, M., Bonifacio, P., Molaro, P., & Vladilo, G. 2000, ApJ, 536, 540
Charlot, S., & Fall, S. M. 1991, ApJ, 378, 471
———. 1993, ApJ, 415, 580
Dekker, H., D'Odorico, S., Kaufer, A., Delabre, B., & Kotzolwski, H. 2000, Proc. SPIE 4008, 534
Dufton, P. L., Keenan, F. P., & Hibbert, A. 1986, A&A, 164, 179
Fedchak, J. A., & Lawler, J. E. 1999, ApJ, 523, 734
Federman, S. R., Beideck, D. J., Schectman, R. M., & York, D. G. 1992, ApJ, 401, 367
Fitzpatrick, E. L. 1996, ApJ, 473, L55
Friedman, S. D., et al. 2000, ApJ, in press (astro-ph/0005459)
Giardino, G., & Favata, F. 2000, A&A, 360, 846
Giavalisco, M., Macchetto, F. D., & Sparks, W. B. 1994, A&A, 288, 103
Grevesse, N., Noels, A., & Sauval, A. J. 1996, in ASP Conf. Ser. 99, Cosmic Abundances (San Francisco: ASP), 117
Henry, R. B. C., & Worthey, G. 1999, PASP, 111, 919
Howk, J. C., Sembach, K. R., Roth, K. C., & Kruk, J. W. 2000, ApJ, 544, 867
Israelian, G., García López, R. G., & Rebolo, R. 1998, ApJ, 507, 805
Izotov, Yu. I., & Thuan, T. X. 1999, ApJ, 511, 639
Jenkins, E. B., Savage, B. D., & Spitzer, L., Jr. 1986, ApJ, 301, 355
Junkkarinen, V. T., Beaver, E. A., Burbidge, E. M., Cohen, R. D., Hamman, F., & Lyons, R. W. 1997, in ASP Conf. Ser. 128, Mass Ejection from Active Galactic Nuclei (San Francisco: ASP), 220
Jura, M., & York, D. G. 1978, ApJ, 219, 861
Kniazev, A. Yu., Pustilnik, S. A., Ugryumov, A. V., & Kniazeva, T. F. 2000, Astrophys. Lett., 26, 129
Kulkarni, V., Fall, S. M., & Truran, J. W. 1997, ApJ, 484, L7
Launay, J. M., & Roueff, E. 1977, A&A, 56, 289
Levshakov, S. A., Agafonova, I. I., & Kegel, W. H. 2000a, A&A, 360, 833
Levshakov, S. A., Chaffee, F. H., Foltz, C. B., & Black, J. 1992, A&A, 262, 385
Levshakov, S. A., Molaro, P., Centurión, M., D'Odorico, S., Bonifacio, P., & Vladilo, G. 2000b, A&A, 361, 803 (Paper II)
Limongi, M., Straniero, O., & Chieffi, A. 2000, ApJS, 129, 625
Lu, L., Sargent, W. L. W., Barlow, T. A., Churchill, C. W., & Vogt, S. 1996, ApJS, 107, 475
McWilliam, A. 1997, ARA&A, 35, 503
Molaro, P., Bonifacio, P., Centurión, M., D'Odorico, S., Vladilo, G., Santin, P., & Di Marcantonio, P. 2000, ApJ, 541, 54 (Paper I)
Molaro, P., Centurión, M., & Vladilo, G. 1998, MNRAS, 293, L37
Molaro, P., D'Odorico, S., Fontana, A., Savaglio, S., & Vladilo, G. 1996, A&A, 308, 1
Morton, D. C. 1991, ApJS, 77, 119
Nomoto, K., Iwamoto, K., Nakasato, N., Thielemann, F.-K., Brachwitz, F., Tsujimoto, T., Kubo, Y., & Kishimoto, N. 1997, Nucl. Phys. A, 621, 467
Ohl, R. G., Chayer, P., & Moos, H. W. 2000, ApJ, 538L, 950
Outram, P. J., Chaffee, F. H., & Carswell, R. F. 1999, MNRAS, 310, 289
Pettini, M., Ellison, S. L., Steidel, C. C., & Bowen, D.V. 1999, ApJ, 510, 576
Pettini, M., Ellison, S., Steidel, C., Shapley, A. E., & Bowen, D. V. 2000, ApJ, in press (astro-ph/9910131)
Pettini, M., Smith, L. J., King, D. L., & Hunstead, R. W. 1997, ApJ, 486, 665
Press, W. H., Teukolsky, S. A., Vetterling, W. T., & Flannery, B. P. 1992, Numerical Recipes (Cambridge: Cambridge Univ. Press)
Prochaska, J. X., Naumov, S. O., Carney, B. W., McWilliam, A., & Wolfe, A. M. 2000, AJ, 120, 2513
Prochaska, J. X., & Wolfe, A. M. 1999, ApJS, 121, 369
———. 2000, ApJ, 533, L5
Samland, M. 1998, ApJ, 496, 155
Savage, B. D., & Sembach, K. R. 1996, ARA&A, 34, 279
Savaglio, S., Cristiani, S., D'Odorico, S., Fontana, A., Giallongo, E., & Molaro, P. 1997, A&A, 318, 347
Sneden, C., Gratton, R., & Crocker, D. A. 1991, A&A, 246, 354
Sofia, U. J., & Jenkins, E. B. 1998, ApJ, 499, 951
Spitzer, L., Jr., & Jenkins, E. B. 1975, ARA&A, 13, 133
Srianand, R., & Petitjean, P. 1998, A&A, 335, 33
Steidel, C. C., & Hamilton, D. 1992, AJ, 104, 941
Timmes, F. X., Woosley, S. E., & Weaver, T. A. 1995, ApJS, 98, 617 (TWW)
Turner, B. E., Tsuji, T., Bally, J., Guelin, M., & Cernicharo, J. 1990, ApJ, 365, 569
Viegas, S. M. 1995, MNRAS, 276, 268
Vladilo, G. 1998, ApJ, 493, 583
Vladilo, G., Bonifacio, P., Centurión, M., & Molaro, P. 2000, ApJ, 543, 24
Woosley, S. E., & Weaver, T. A. 1995, ApJS, 101, 181

Note added in proof.—When the method introduced here to analyze lines in the Lymanα forest is applied to the O I λ950.8846 and O I 925.4460 transitions discussed in Paper I, improved O abundances are obtained (P. Molaro et al. 2001, in Proc. IAP Melting on Cosmic Chemical Evolution [Paris: IAP], in press). The O I column density is log O I $= 16.27 \pm 0.005$, which implies [O/H] $= 2.01 \pm 0.12$, [O/Zn] $= 0.06 \pm 0.11$, and [O, Ar, S/Fe, Cr, Zn] $= 0.11 \pm 0.014$. The log (Ar/O) and log (S/O) become -2.25 ± 0.06 and $-1.57 \pm$, respectively, i.e., the values are almost identical to the values measured in the blue compact galaxies by Izotov et al. (1999).